ANTICANCER RESEARCH *41*: 4083-4088 (2021)
doi:10.21873/anticanres.15210

# Construction of a Drug Release Evaluation System: Application of Mitochondrial Respiration to Monitor Drug Release

KAZUTO OHKURA[1], YOHEI TATEMATSU[1] and ATSUSHI TABATA[2]

[1]*Graduate School of Pharmaceutical Sciences, Suzuka University of Medical Science, Suzuka, Japan;*
[2]*Department of Biological Science and Technology, Life System, Institute of Technology and Science, Tokushima University Graduate School, Tokushima, Japan*

**Abstract.** *Background/Aim: Efficient drug encapsulation and regulation of drug release are important factors for sustained drug release and application for release-controlled anti-cancer and anti-inflammatory drug delivery. In the present study, a direct evaluation system for drug-release from model carrier (e.g., alginate-gel beads) was examined using the mitochondrial oxygen consumption rate as an index. Materials and Methods: Alginate-gel beads were coated with the uncoupler SF6847 (SF beads) and used as a model microparticle-type drug. The real-time monitoring of SF6847 release from prepared alginate-gel beads was performed using the mitochondrial oxygen consumption rate. Release profiles of nonsteroidal anti-inflammatory drugs [NSAIDs, mefenamic acid (MEF) and diclofenac (DIC)] from alginate-gel beads as well as SF beads were investigated using the real time monitoring system. Results: SF6847 release from alginate-gel beads was clearly detected using the rat liver mitochondrial oxygen consumption rate. The release features of MEF and DIC from alginate-gel beads were defined by the present trial monitoring system, and these NSAIDs exhibited different release profiles. Conclusion: The present drug monitoring system detected released drugs, and the release profile reflected the molecular properties of the test drugs. This system may be applied to the design and development of precise sustained drug release systems (e.g., anti-cancer and anti-inflammatory drugs).*

Microspheres and fine particles called micro- and nanoparticles have been used as drug carriers in the development of drug delivery systems (DDS). The behavior of these particles may be controlled by adjusting their size and surface properties (*e.g.*, hydrophobicity, charge, and chemical modifications). Their binding affinities for target molecules may also be controlled by introducing specific ligands to their surfaces. Liposomes are one of the most frequently used drug carriers (1), and immunoliposomes (2, 3), amphisomes (4), proteoliposomes (5), peptide-tagged liposomes (6-9), and lectin-modified liposomes (10) have also been employed.

The aim of drug delivery using microparticle carriers such as liposomes, is to release a drug at its target site. These microparticles cannot sufficiently exert their function simply by reaching the target site, and, thus, an appropriate drug concentration needs to be maintained at the target site. The construction of a real-time drug release monitoring system is very useful for efficient DDS formulations. The controlled release of active agents (*e.g.*, anti-cancer drugs and hepatotoxic drugs) is important for improving the quality of life of patients. In experiments on drug-induced liver injury (DILI), we previously demonstrated that mitochondria responded sensitively to several mitochondrial inner membrane permeability transition-inducing drugs and showed rapid oxygen consumption (11, 12). In the present study, we developed a real-time drug release monitoring system using the mitochondrial oxygen consumption rate. Release properties from the carrier were used as an index to measure the utility of the drug delivery system. Therefore, we investigated the release of encapsulated drugs from the carrier matrix using a directly detectable system. Drug carrier alginate gel beads were prepared and the release profiles of uncoupling agents (*e.g.*, SF6847, MEF, and DIC), which exert an uncoupling effect on the electron transport chain of the mitochondrial inner membrane, were examined using mitochondrial oxygen consumption rate as an index.

## Materials and Methods

Preparation of SF6847-encapsulated alginate gel beads. SF6847 was added to a 1% (w/v) sodium alginate solution containing 25% (v/v) DMSO to a final concentration of 20 μM and then completely mixed. One milliliter of the solution was dropped into gelatinization solution [0.3M $CaCl_2$, 25%(v/v) DMSO] using a syringe equipped with 21G needle, and then incubated for the specified time (5, 10, 30, and 60 min) at room temperature. The SF-beads prepared were

Correspondence to: Prof. Kazuto Ohkura, Graduate School of Pharmaceutical Sciences, Suzuka University of Medical Science, 3500-3 Minamitamagaki-cho, Suzuka, Mie 513-8670, Japan. Tel: +81 593400611, Fax: +81 593681271, e-mail: kohkura@suzuka-u.ac.jp

Key Words: Drug release, drug monitoring, mitochondrial respiration.

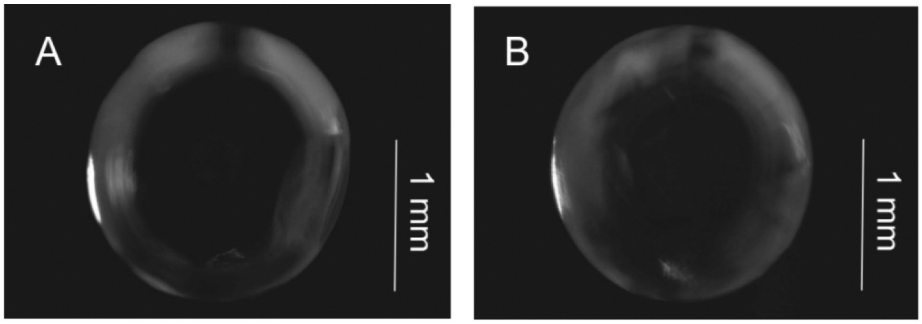


Figure 1. *Alginate-gel bead. Prepared alginate-gel beads were observed by an inverted microscope (CKX41, Olympus, Tokyo, Japan). A) control alginate-gel bead without SF6847 (control bead). B) SF6847 encapsulated alginate-gel bead (SF bead).*

briefly rinsed with ultra-pure water and then used after the removal of excess fluid. The amount of SF6847 in the alginate-gel beads was evaluated based on the measurement of the absorbance at 450 nm ($A_{450}$) of the solution for alginate-gel beads preparation. Briefly, after the preparation of alginate-gel beads the $A_{450}$ of gelatinization solution was measured, and the concentration of SF6847 was assessed based on the standard curve for SF6847 concentration against $A_{450}$. After calculation the concentration of SF6847 in the gelatinization solution, encapsulation efficiency was evaluated.

*Monitoring of SF6847 release from alginate-gel beads*. The real-time monitoring of SF6847 release from alginate-gel beads was performed using the mitochondrial oxygen consumption as an index. Isolation of mitochondria from the rat liver was conducted as previously described (13, 14). Mitochondria were incubated in inorganic Pi-containing medium [+Pi medium: 200 mM sucrose, 10 mM $K_3PO_4$-$KH_2PO_4$ (K/Pi) buffer, pH 7.4] at a final protein concentration of 0.7 mg/ml, and energized by 10 mM succinate, 1 μg/ml rotenone, and 2 μM ruthenium red (RR: calcium uniporter inhibitor). Freshly prepared SF-beads were added to the mitochondrial suspension, and mitochondrial oxygen consumption was monitored using the Clark oxygen electrode (Yellow Spring 5331, Yellow Springs Instrument Co. Inc., Yellow Springs, OH, USA). The velocity of mitochondrial oxygen consumption was monitored, and the amount of SF6847 released was assessed using the oxygen consumption rate. The relationship between the concentration of SF6847 and the oxygen consumption rate was investigated.

*Real-time monitoring of drug release from alginate-gel beads*. Mefenamic acid (MEF)- or diclofenac (DIC)-encapsulated alginate-gel beads (designated as NSAIDs-beads) were prepared as well as SF-bead preparation, and sodium alginate solution was mixed with NSAIDs [10 mM MEF or 10 mM DIC in 1% (w/v) sodium alginate solution containing 5% (v/v) DMSO]. The NSAID-beads were added to the mitochondrial suspension, and the release of encapsulated NSAIDs was evaluated using the mitochondrial oxygen consumption rate with a Clark oxygen electrode.

## Results

*Characteristics of SF6847-encapsulated alginate-gel beads*. The alginate-gel beads prepared were spherical with a diameter of 1.5 mm, and no significant differences were observed in their shape or size with or without SF6847 encapsulation (Figure 1). The shape and size of the alginate-gel beads prepared did not change following incubation at 25˚C for 20 min. The gelling time of SF6847-encapsulated beads affected the encapsulation efficiency of SF6847, with efficiency of 51.1% in a 5-min gelling time. Efficiency decreased to 19.2% with 30-min gelling-time, and was unchanged by a 60-min gelling-time (Figure 2).

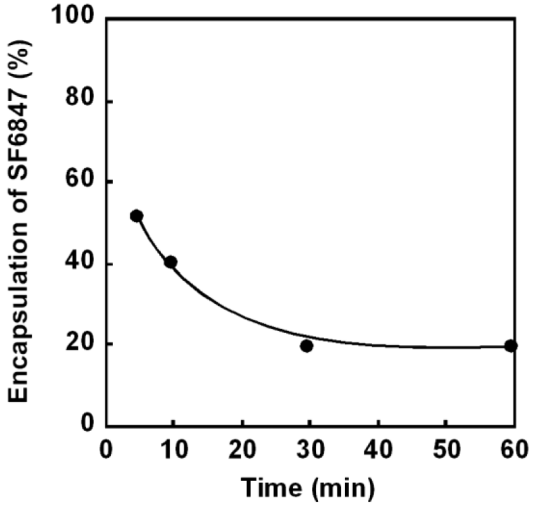


Figure 2. *Effect of gelling time on the encapsulation efficiency of SF6847. The encapsulation efficiency at each gelling time (5, 10, 30, and 60 min) was determined based on SF6847remained in the gelling solution.*

*Real-time monitoring of SF6847 release from alginate-gel beads*. The alginate-gel beads prepared enhanced mitochondrial oxygen consumption (c: SF6847-free control beads in Figure 3A) because control beads were constructed using calcium (0.3 M $CaCl_2$)-containing gelatinization solution, and calcium-induced mitochondrial permeability

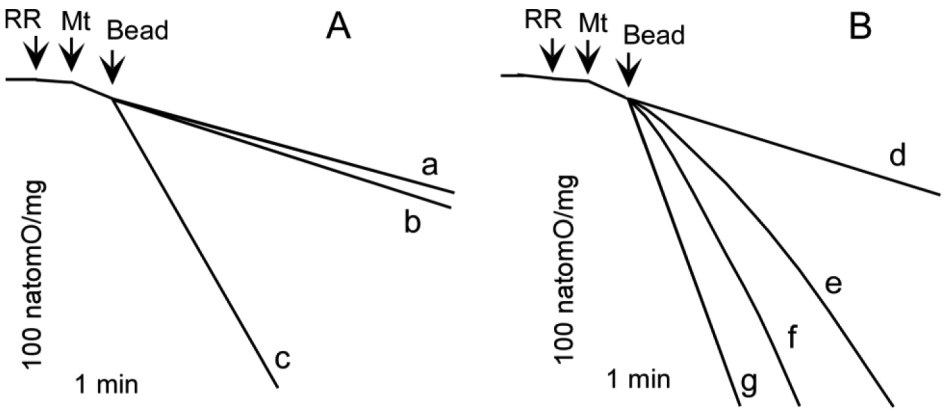


Figure 3. *Real-time monitoring of SF6847 release from alginate-gel beads. Mitochondria (Mt) were suspended at a final protein concentration of 0.7 mg/ml in +Pi medium supplemented with 10 mM succinate and 1 μg/ml rotenone as respiratory substrates, and the change in dissolved oxygen was monitored using Clark oxygen electrode (Yellow Spring 5331). A) Mitochondrial oxygen consumption in the presence of 2 μM Ruthenium red (RR) (a), in the absence of alginate beads (b), in the presence of SF6847 free beads (control beads) without RR pretreatment (c). B) Mitochondrial oxygen consumption with control beads in the presence of 2 μM RR (d), SF beads (10 min gelling) (e), SF beads (5 min gelling) (f), and SF6847 (100 nM) (g).*

transition then occurred. Control beads-induced mitochondrial oxygen consumption was suppressed by the calcium uniporter inhibitor ruthenium red (RR) (a: 2 μM RR pretreatment in Figure 3A). In the absence of control beads (b), the mitochondrial oxygen consumption rate was similar to that in the RR-pretreated condition (a).

In the RR (2 μM)-pretreated condition, the addition of SF beads with a gelling time of 5 min (Figure 3B) (f) or 10 min (e) enhanced mitochondrial oxygen consumption more than that of control beads (d). The oxygen consumption rate was significantly increased by the addition of SF6847 (100 nM) (g).

*Relationship between SF6847 concentration and oxygen consumption*. The oxygen consumption rate increased in a SF6847 concentration-dependent manner (Figure 4A). The oxygen consumption rate with the addition of 100 nM SF6847 was set to 100%, and the oxygen consumption ratio of each SF6847 concentration was obtained (Figure 4B). The oxygen consumption rate increased in a SF6847 dose-dependent manner until 25 nM. At concentrations higher than 25 nM, the oxygen consumption rate reached 100%.

Based on the relationship between the concentration of SF6847 and the oxygen consumption rate, the time course of SF6847 release from SF beads was elucidated (Figure 5). The release profile of SF6847 from SF beads was dependent on the gelling conditions, with release being more gradual from beads with a gelling time of 10 min (b) than 5 min (a).

*Real-time monitoring of NSAID release from alginate-gel beads*. MEF and DIC exhibited mitochondrial uncoupling activities as SF6847, and dose-dependently enhanced mitochondrial oxygen consumption (MEF: 0-30 μM and DIC: 0-100 μM) (11). The real-time monitoring of MEF and DIC release from alginate-gel beads was performed using mitochondrial oxygen consumption, and the gradual elution of MEF from MEF-encapsulated beads was observed (open circles in Figure 6). On the other hand, DIC was rapidly eluted from the DIC-encapsulated beads (closed circles). The release features of the NSAIDs tested from encapsulated alginate-gel beads were assigned by the mitochondria applied drug monitoring system.

## Discussion

We herein attempted to construct a system for evaluating drug release from pharmaceuticals using mitochondrial response to the drugs released. Alginic acid-gel beads were prepared by gelling alginic acid, a polysaccharide contained in brown algae, and the beads obtained were then used as a drug carrier model. The SF6847 elution profile from SF6847-encapsulated alginate-gel beads (SF beads) was measured using the mitochondrial oxygen consumption rate as an index (15, 16). The release of SF6847 from SF beads was directory detectable in the present monitoring system. The gelation time affected the amount of SF6847 taken up into the gel, and the mitochondrial oxygen consumption rate varied depending on the gelation time. The encapsulation amounts of drugs may be regulated by controlling the gelation time. Surface-dried SF beads exhibited a slower release of SF6847 than undried SF beads. The SF6847 release rates of dried SF beads were 10.1 % (gelation time of 5 min) or 37.7% (gelation time of 10 min) lower than those of undried SF beads (data not shown). The gel surface became dry and hard, and the release of SF6847 was delayed.

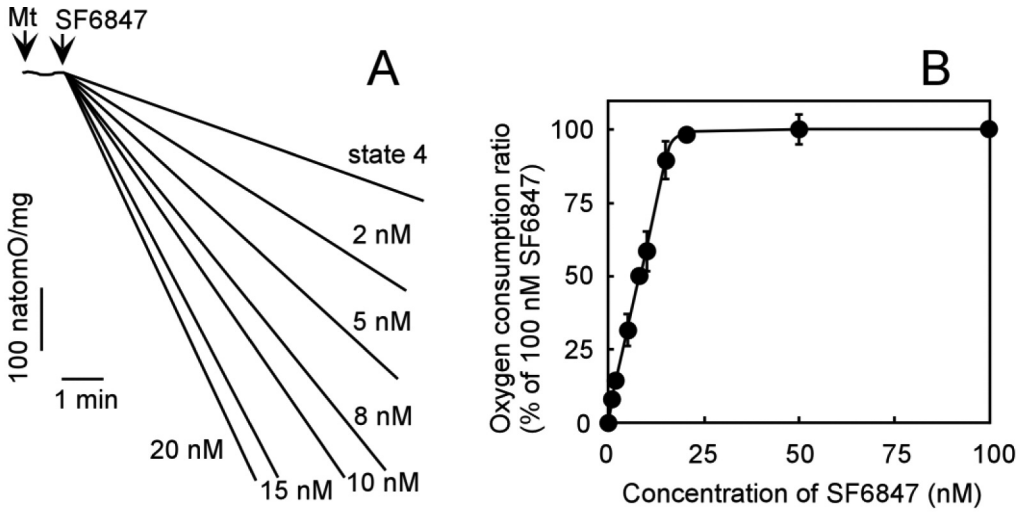


Figure 4. *SF6847 dependent mitochondrial oxygen consumption. Mitochondrial oxygen consumption rate was monitored as in Figure 3. The basal oxygen consumption rate (state 4) was 25.8±1.6 atoms O/mg/min. Oxygen consumption in the presence of SF6847 (2, 5, 8, 10, 15, and 20 nM) is shown (A). The consumption rate in the presence of 100 nM SF6847 was set to 100%, and the rate at each SF6847 concentration is plotted (B). Results represent the mean±standard error obtained from 3 independent experiments.*

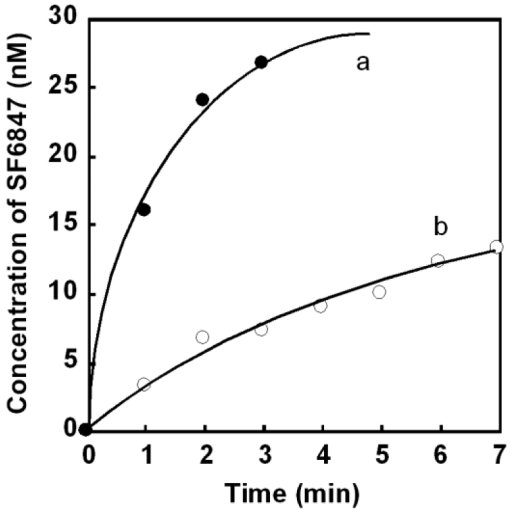


Figure 5. *Time course of SF6847 release from SF beads. SF6847 release from SF beads after 5 min (closed circles), 10 min (open circles) gelling was monitored, and released SF6847 was calculated as in Figure 4B.*

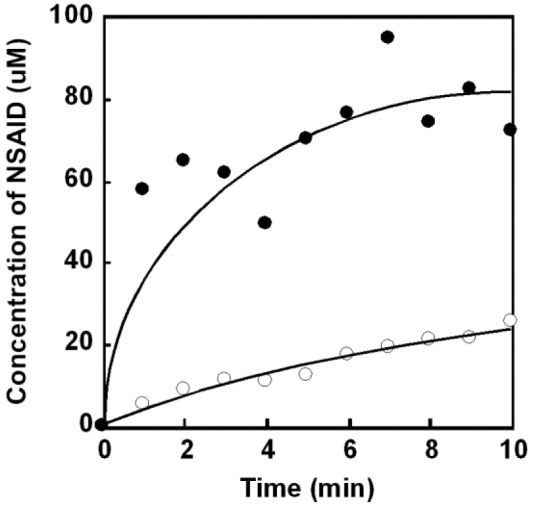


Figure 6. *Real-time monitoring of NSAID release from alginate-gel beads. Elution profile of NSAID (open circles: MEF, closed circles: DIC) was determined using the mitochondrial oxygen consumption rate. Concentration of each eluted NSAID was calculated every min using the calibration curve of each NSAID as well as SF6847.*

The release of pharmaceuticals that promote mitochondrial oxygen consumption, such as MEF and DIC, from a carrier may be directly evaluated. NSAID-encapsulated alginate-gel beads (MEF or DIC beads) were prepared, and the release features were analyzed using mitochondrial oxygen consumption as an index. Gradual MEF release and rapid DIC release from alginate-gel beads were observed. Furthermore, drug release from gel beads was affected by the type of encapsulated drug. The release profiles of MEF and DIC from other types of drug delivery

carriers are currently being examined. The strategy of utilizing the release profiles of interacting drugs from drug delivery carrier is applicable to any drug combination, such as anticancer drugs. Thus, a very beneficial dosing system may be constructed. Even if drugs are simultaneously administered, side effects may be avoided based on the carrier selected, which may contribute to improvements in the quality of life of patients.

The hydrophobicity of a drug is an important factor affecting its ability to penetrate cell membranes and alginate gels. Stereohydrophobicity (solvation free energy dGW) (a lower dGW value means higher hydrophobicity) was previously identified as a parameter for assessing the degree of hydrophobicity derived from the three-dimensional structure of a molecule (17-19). SF6847, a powerful uncoupler, has excellent mobility in membranes and functions as a protonophore. The dGW of SF6847 has been examined using a conformational analysis, and the average value obtained was –62.92 kJ/mol, which remained constant regardless of conformational changes (11). During the conformation analysis, the dGW value of MEF significantly changed, and the majority of MEF conformers showed larger dGW values than the average dGW value of SF6847 (11). The membrane effects of these MEF conformers are considered to be weak. DIC showed a dGW value near or below the average dGW value of SF6847 regardless of its conformation (11), and DIC exerted similar membrane effects to SF6847 in any conformation. DIC penetrated the membrane in any conformation, and its elution from alginate-gel beads was rapid due to its properties. Regarding MEF, only conformations showing appropriate hydrophobicity penetrate the alginate gel, and slow elution from alginate-gel beads was observed.

The system for evaluating drug release using mitochondrial function may be employed to elucidate the characteristics of drug carriers in detail. Even for a drug that does not exert an uncoupling effect, release from a carrier may be detected by including a probe that controls the proton gradient. We are now conducting research to design and develop this probe.

## Conflicts of Interest

The Authors declare no conflicts of interest regarding this study.

## Authors' Contributions

Kazuto Ohkura, Yohei Tatematsu and Atsushi Tabata carried out the experiment. All Authors provided critical feedback and helped shape the research, analysis and manuscript.

## Acknowledgements

This work was supported, in part, by a Grant-in-Aid for Scientific Research (18K06764) (21K06655) from the Ministry of Education, Culture, Sports, Science and Technology of the Japanese Government.

## References

1 Langer R: New methods of drug delivery. Science *249(4976)*: 1527-1533, 1990. PMID: 2218494. DOI: 10.1126/science.2218494

2 Hatakeyama H, Akita H, Ishida E, Hashimoto K, Kobayashi H, Aoki T, Yasuda J, Obata K, Kikuchi H, Ishida T, Kiwada H and Harashima H: Tumor targeting of doxorubicin by anti-MT1-MMP antibody-modified PEG liposomes. Int J Pharm *342(1-2)*: 194-200, 2007. PMID: 17583453. DOI: 10.1016/j.ijpharm.2007.04.037

3 Nishikawa K, Asai T, Shigematsu H, Shimizu K, Kato H, Asano Y, Takashima S, Mekada E, Oku N and Minamino T: Development of anti-HB-EGF immunoliposomes for the treatment of breast cancer. J Control Release *160(2)*: 274-280, 2012. PMID: 22020380. DOI: 10.1016/j.jconrel.2011.10.010

4 Puri A, Kramer-Marek G, Campbell-Massa R, Yavlovich A, Tele SC, Lee SB, Clogston JD, Patri AK, Blumenthal R and Capala J: HER2-specific affibody-conjugated thermosensitive liposomes (Affisomes) for improved delivery of anticancer agents. J Liposome Res *18(4)*: 293-307, 2008. PMID: 18937120. DOI: 10.1080/08982100802457377

5 Hwang SY, Cho DY, Kim HK, Cho SH, Choo J, Yoon WJ and Lee EK: Preparation of targeting proteoliposome by postinsertion of a linker molecule conjugated with recombinant human epidermal growth factor. Bioconjug Chem *21(2)*: 345-351, 2010. PMID: 20078100. DOI: 10.1021/bc9004409

6 Shahin M, Soudy R, El-Sikhry H, Seubert JM, Kaur K and Lavasanifar A: Engineered peptides for the development of actively tumor targeted liposomal carriers of doxorubicin. Cancer Lett *334(2)*: 284-292, 2013. PMID: 23073474. DOI: 10.1016/j.canlet.2012.10.007

7 Terada T, Mizobata M, Kawakami S, Yamashita F and Hashida M: Optimization of tumor-selective targeting by basic fibroblast growth factor-binding peptide grafted PEGylated liposomes. J Control Release *119(3)*: 262-270, 2007. PMID: 17467100. DOI: 10.1016/j.jconrel.2007.01.018

8 Wang Z, Yu Y, Dai W, Lu J, Cui J, Wu H, Yuan L, Zhang H, Wang X, Wang J, Zhang X and Zhang Q: The use of a tumor metastasis targeting peptide to deliver doxorubicin-containing liposomes to highly metastatic cancer. Biomaterials *33(33)*: 8451-8460, 2012. PMID: 22940213. DOI: 10.1016/j.biomaterials.2012.08.031

9 Yan Z, Yang Y, Wei X, Zhong J, Wei D, Liu L, Xie C, Wang F, Zhang L, Lu W and He D: Tumor-penetrating peptide mediation: an effective strategy for improving the transport of liposomes in tumor tissue. Mol Pharm *11(1)*: 218-225, 2014. PMID: 24325555. DOI: 10.1021/mp400393a

10 Bakowsky H, Richter T, Kneuer C, Hoekstra D, Rothe U, Bendas G, Ehrhardt C and Bakowsky U: Adhesion characteristics and stability assessment of lectin-modified liposomes for site-specific drug delivery. Biochim Biophys Acta *1778(1)*: 242-249, 2008. PMID: 17964278. DOI: 10.1016/j.bbamem.2007.09.033

11 Tatematsu Y, Hayashi H, Taguchi R, Fujita H, Yamamoto A and Ohkura K: Effect of N-phenylanthranilic acid scaffold nonsteroidal anti-inflammatory drugs on the mitochondrial permeability transition. Biol Pharm Bull *39(2)*: 278-284, 2016. PMID: 26830486. DOI: 10.1248/bpb.b15-00717

12 Tatematsu Y, Fujita H, Hayashi H, Yamamoto A, Tabata A, Nagamune H and Ohkura K: Effects of the nonsteroidal anti-inflammatory drug celecoxib on mitochondrial function. Biol Pharm Bull *41(3)*: 319-325, 2018. PMID: 29491208. DOI: 10.1248/bpb.b17-00527

13 Yamada A, Yamamoto T, Yamazaki N, Yamashita K, Kataoka M, Nagata T, Terada H and Shinohara Y: Differential permeabilization effects of $Ca^{2+}$ and valinomycin on the inner and outer mitochondrial membranes as revealed by proteomics analysis of proteins released from mitochondria. Mol Cell Proteomics *8(6)*: 1265-1277, 2009. PMID: 19218587. DOI: 10.1074/mcp.M800377-MCP200

14 Kawashima S, Yamamoto T, Horiuchi Y, Fujiwara K, Gouda S, Yoshimura Y, Yamamoto A, Inotani Y, Yamashita K, Kitamura S, Terada H, Kanematsu M, Shishido K and Shinohara Y: S-15176 and its methylated derivative suppress the CsA-insensitive mitochondrial permeability transition and subsequent cytochrome c release induced by silver ion, and show weak protonophoric activity. Mol Cell Biochem *358(1-2)*: 45-51, 2011. PMID: 21688046. DOI: 10.1007/s11010-011-0919-x

15 Kamoun E: Alginate hydrogel as drug delivery system: Preparation of alginate hydrogel and its application as drug delivery system. VDM Verlag Dr. Mueller, 2010.

16 Lopes M, Abrahim B, Veiga F, Seiça R, Cabral LM, Arnaud P, Andrade JC and Ribeiro AJ: Preparation methods and applications behind alginate-based particles. Expert Opin Drug Deliv *14(6)*: 769-782, 2017. PMID: 27492462. DOI: 10.1080/17425247.2016.1214564

17 Ohkura K and Hori H: Analysis of structure-permeability correlation of nitrophenol analogues in newborn rat abdominal skin using semiempirical molecular orbital calculation. Bioorg Med Chem *7(2)*: 309-314, 1999. PMID: 10218822. DOI: 10.1016/s0968-0896(98)00200-4

18 Ohkura K, Sukeno A, Yamamoto K, Nagamune H, Maeda T and Kourai H: Analysis of structural features of bis-quaternary ammonium antimicrobial agents 4,4'-(alpha,omega-polymethylenedithio)bis (1-alkylpyridinium iodide)s using computational simulation. Bioorg Med Chem *11(23)*: 5035-5043, 2003. PMID: 14604666. DOI: 10.1016/j.bmc.2003.08.027

19 Ohkura K, Sukeno A, Nagamune H and Kourai H: Bridge-linked bis-quaternary ammonium anti-microbial agents: relationship between cytotoxicity and anti-bacterial activity of 5,5'-[2,2'-(tetramethylenedicarbonyldioxy)-diethyl]bis(3-alkyl-4-methylthiazonium iodide)s. Bioorg Med Chem *13(7)*: 2579-2587, 2005. PMID: 15755659. DOI: 10.1016/j.bmc.2005.01.030

*Received May 21, 2021*
*Revised June 6, 2021*
*Accepted June 7, 2021*